THE PROBLEM OF CONVECTIVE MOISTENING

Kerry A. Emanuel
Program in Atmospheres, Oceans, and Climate
Massachusetts Institute of Technology
Cambridge, Massachusetts, USA

1. INTRODUCTION

Convective representations strive to simulate, in a realistic way, convective precipitation and the feedback of convection upon the explicitly simulated flow. The prediction of convective precipitation and convective heating are of obvious importance and a great deal of work has been devoted to improving and evaluating the fidelity with which convective schemes reproduce these quantities. Historically, the moistening of the atmosphere by convection has been of secondary concern, perhaps because it is not obviously of great importance to very short range weather prediction. On the other hand, it must become an increasingly important concern as the range of the forecast increases, while it is arguably among the most important problems in climate simulations, given that water vapor is the most important feedback mechanism in virtually all climate simulations performed to date.

My purpose here is first to show that "traditional" methods of evaluating convective moistening have serious limitations, and then to propose and demonstrate another technique for evaluating the fidelity of the representation of convective moistening. In the process, I will briefly introduce a new representation of cumulus convection.

2. EVALUATING CONVECTIVE MOISTENING (AND HEATING)

One "traditional" approach alluded to above is the semi-prognostic test, introduced by Lord (1982) using the diagnostic methodology developed by Yanai et al. (1973). Briefly, the ensemble-averaged equations for liquid water virtual static energy (e.g., see Emanuel, 1994) and specific humidity can be written

$$\frac{\partial \overline{h}_{lv}}{\partial t} + \overline{\mathbf{V}}_H \cdot \nabla \overline{h}_{lv} + \overline{w}\frac{\partial \overline{h}_{lv}}{\partial z} - \overline{\dot{R}} = Q_1, \tag{2.1}$$

$$\frac{\partial \overline{q}}{\partial t} + \overline{\mathbf{V}}_H \cdot \nabla \overline{q} + \overline{w}\frac{\partial \overline{q}}{\partial z} = -\frac{Q_2}{L_v}, \tag{2.2}$$

where h_{lv} is the liquid water virtual static energy given by

$$h_{lv} \equiv [c_{pd}(1-q) + c_{pv}q]T + gz - L_v l, \tag{2.3}$$

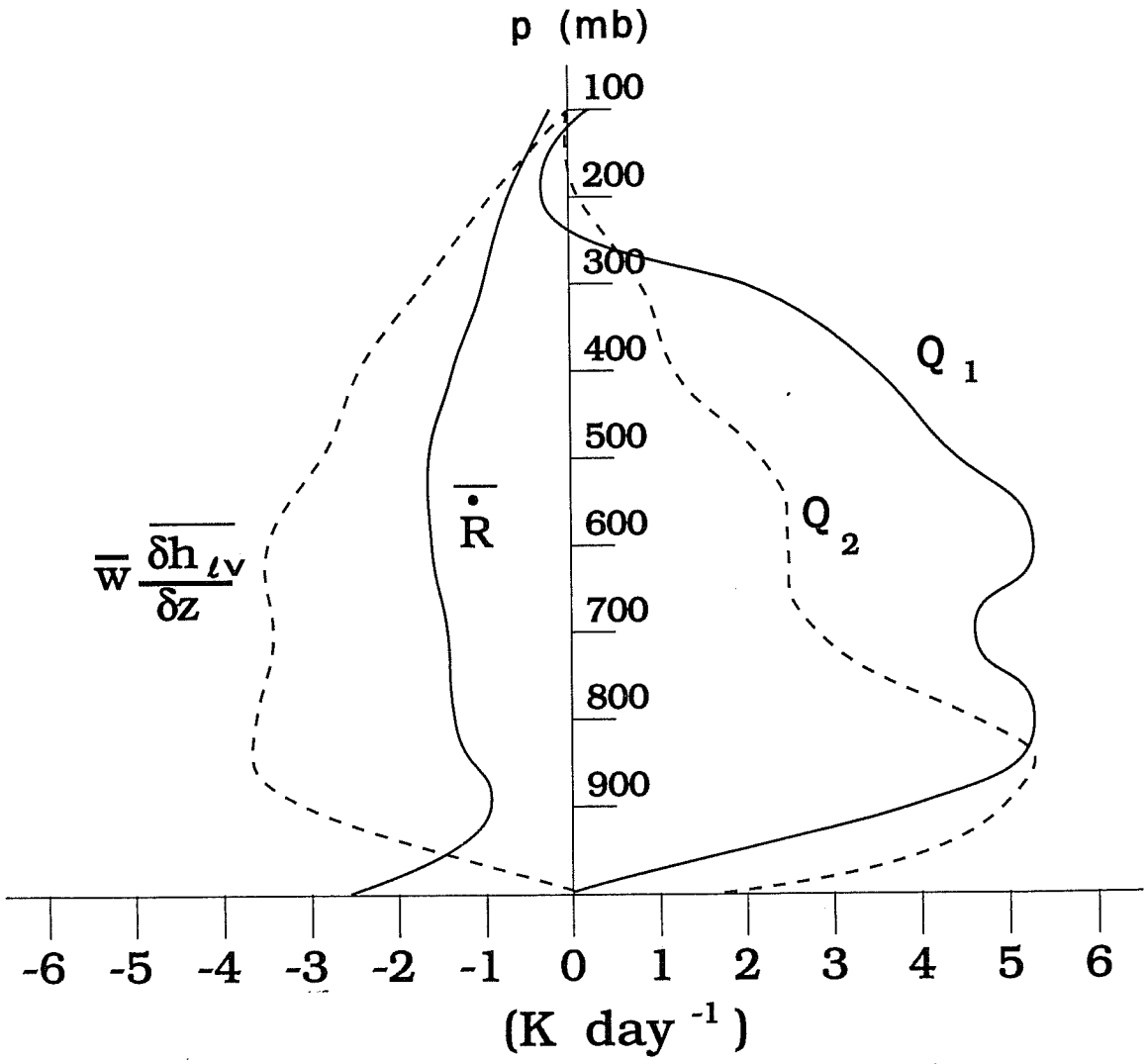

Fig. 1 Average values of Q_1, Q_2, adiabatic cooling and radiative cooling during Phase 3 of GATE.

q is the specific humidity, l is the liquid water content, $\overline{\mathbf{V}}_H$ is the vector horizontal wind, w is the vertical velocity, $\overline{\dot{R}}$ is the radiative heating, and L_v is the latent heat of vaporization. The overbars represent cumulus ensemble averages. Q_1 and Q_2 are referred to as the apparent heat source and apparent moisture sink, respectively, and subsume all the subensemble turbulent transports, which are assumed to be dominated by moist convection when it occurs (except in the subcloud layer).

The left-hand sides of (2.1) and (2.2) can be evaluated from synoptic-scale sounding arrays such as the Inner Flux Array operated during TOGA COARE, with the radiative heating and surface fluxes either observed or calculated using various methods. Thus Q_1 and Q_2 can be deduced as residuals of (2.1) and (2.2). An example of this kind of calculation, made for all of phase 3 of GATE, is shown in Figure 1.

In the semi-prognostic test, a single-column model incorporating a convective representation is essentially integrated for one or a very limited number of time steps, driven by ensemble-averaged vertical motion, radiation, horizontal advection, and surface fluxes provided by the sounding array

data (e.g., the GATE data used to derive Figure 1). The convective scheme "predicts" Q_1 and Q_2, and these can be compared to their diagnosed values. An example of such comparisons is shown in Figure 2.

The problem with using this technique to evaluate convective schemes is immediately evident on examining Figure 2 and noting that *typical values of* $\partial T/\partial t$ *and* $\frac{L_v}{c_p}\frac{\partial q}{\partial t}$ (where c_p is the heat capacity at constant pressure) *are of the order of* $0.1°C/day$ *in the tropics.* Thus the actual tendencies, which are what one is trying to obtain, represent small residuals between advection, radiation, and Q_1 (or Q_2). The apparent fidelity of the convective representation of Q_1 and Q_2 as seen in Figure 2 is a chimera; the differences between observed and predicted Q_1 (or Q_2) yield temperature and moisture tendencies at least an order of magnitude greater than observed. By this type of measure, virtually all schemes fail semi-prognostic tests rather miserably.

In fact, by a proper evaluation of semi-prognostic tests, cumulus parameterization would appear to be a badly losing proposition. The same problem exists when convective precipitation is compared to observed precipitation, since precipitation is simply a vertical integral of Q_2. Thus a scheme that makes an instantaneous error of only 10% in convective precipitation easily can be getting moisture tendencies wrong by factors of 10.

On the other hand, convective schemes seem to perform well by other measures when used in the normal fully prognostic mode. The reason for this is straightforward: although tendencies produced by convective schemes during the first few time steps of an integration can be (and typically are) off by a very large factor, the model thermodynamic fields adjust quite rapidly to this sad state of affairs and thereafter the scheme and the model live in mutual harmony for the rest of the integration, rather like strangers acclimatizing themselves to an arranged marriage. That this must be the case is amply demonstrated by the observation that model simulated temperature tendencies in convecting atmospheres are very small, just as in nature, and nowhere near the magnitude implied by the residuals in Figure 2.

Thus the failure of all schemes to pass semi-prognostic tests is really a failure of the test, leaving us with no evaluation, one way or another, of the scheme.

The other traditional approach to evaluating convective schemes is also flawed. This involves inserting a new scheme in a forecast model and comparing the quality of forecasts to those produced by the model using other convective schemes. This would be a valid approach if it were true that the convective scheme is the dominant source of error in numerical weather prediction. If it is not the dominant error source (or if other error sources are of comparable magnitude to that of the convective scheme), then a better forecast may simply indicate a better degree to which the convective scheme in question compensates for other systematic errors. It could perhaps be argued that the "fully predictive" method would be a valid means of comparing convective schemes if, each time a new

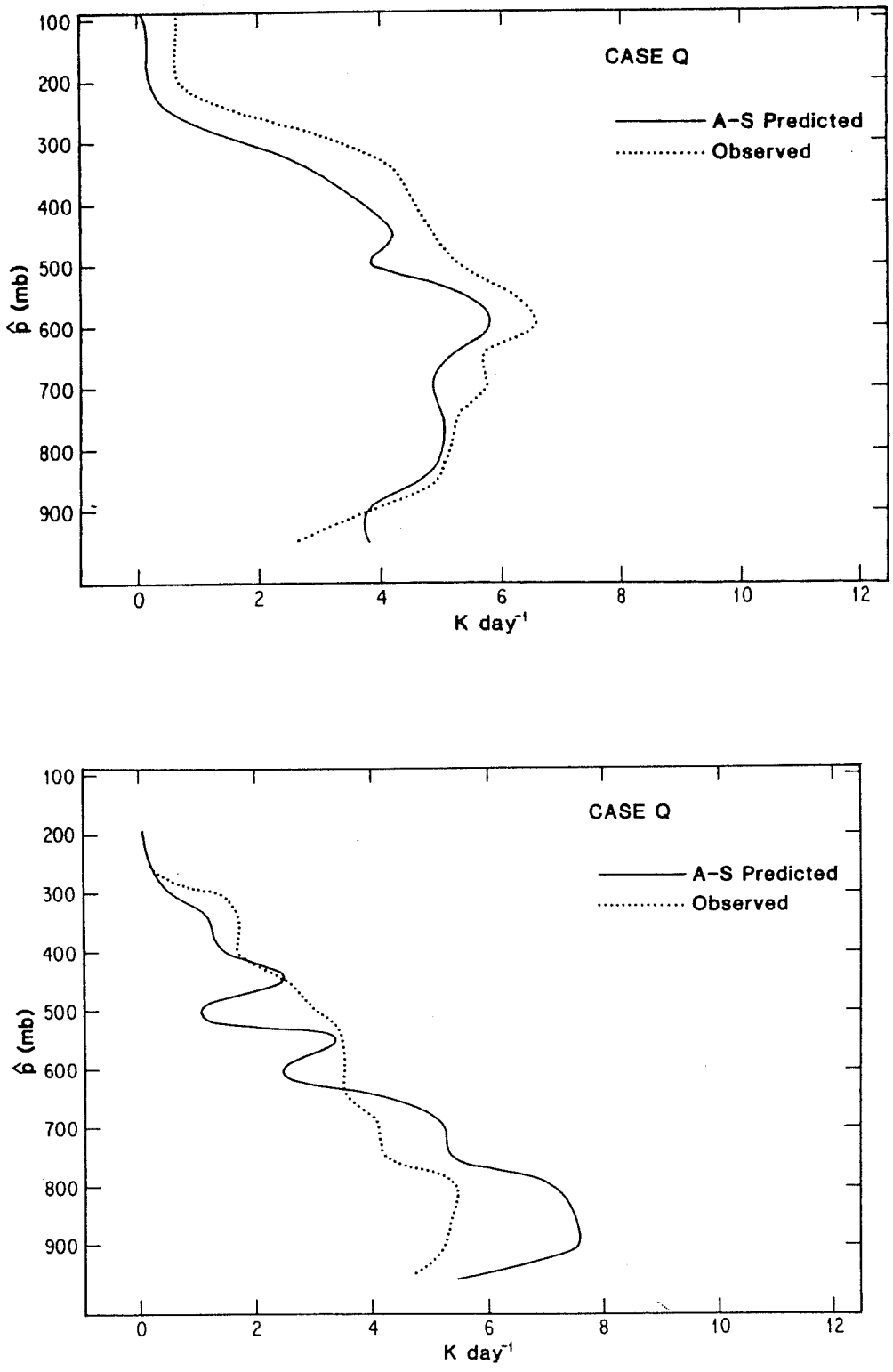

Fig. 2 Values of Q_1 (top) and Q_2 bottom predicted by the Arakawa-Schubert scheme (solid) and diagnosed from data (dotted). From Lord (1982).

scheme is tried, the entire model is globally re-optimized with respect of *all* its adjustable parameters, but to do this would be prohibitively expensive.

3. EFFECTIVE EVALUATION OF CONVECTIVE REPRESENTATIONS

Clearly, an effective evaluation of a convective representation requires integration over a reasonable period of time. (I will argue presently that a "reasonable" period of time is *at least* 20 days.) On the other hand, it is highly desirable to isolate errors in convective schemes from other sources of error in large model integrations. A reasonable compromise is to drive a single-column model with observed forcing over an extended period of time, and compare a *sensitive* predictand to observations. As will be demonstrated shortly, one such sensitive predictand is relative humidity, which is also to a good approximation, the relevant moisture variable for radiative transfer. It turns out to be very easy to get the relative humidity wrong, and this is a good indication that it is a strong test for convective schemes.

Thus one effective means of evaluating convective representations is to predict relative humidity in a single-column model driven over a long period of time by "observed" forcing. The model equations are similar to (2.1) and (2.2):

$$\frac{\partial h_{lv}}{\partial t} = -[\mathbf{V}_H \cdot \nabla h_{lv}] - [w]\frac{\partial h_{lv}}{\partial z} + \dot{R} + [F_{h_{lv}}] + C_{h_{lv}}, \tag{3.1}$$

$$\frac{\partial q}{\partial t} = -[\mathbf{V}_H \cdot \nabla q] - [w]\frac{\partial q}{\partial z} + [F_q] + C_q. \tag{3.2}$$

Here, the bracketed terms are assessed from sounding array data. The F terms in (3.1) and (3.2) represent surface fluxes while the C terms are the convective tendencies provided by the convection scheme that is being assessed. From the time evolution of h_{lv} and q, the relative humidity evolution can be diagnosed.

Over what period of time should the integration of (3.1) and (3.2) be carried out? Here it is important to discuss the physics of convective adjustment. The buoyancy adjustment is physically carried out by internal gravity-inertia waves and occurs over a time scale representing the time it takes the group velocity of such waves to traverse either a typical intercloud spacing or a deformation radius, whichever is smaller. The time scale works out to be of the order of 6 hours. On the other hand, most of the water vapor adjustment occurs by actual mass transport, and the limiting time scale here is the time it takes clear air to subside through the cloud layer, in between clouds. This is more like 20 days. Thus, we cannot expect the water vapor field to equilibrate to a convection scheme over a time much smaller than 20 days, and (3.1)–(3.2) should therefore be integrated for *at least* 20 days.

Figure 3 shows the adjustment of middle tropospheric temperature and water vapor with time in a single-column integration from an arbitrary initial state into a state of strict radiative-convective

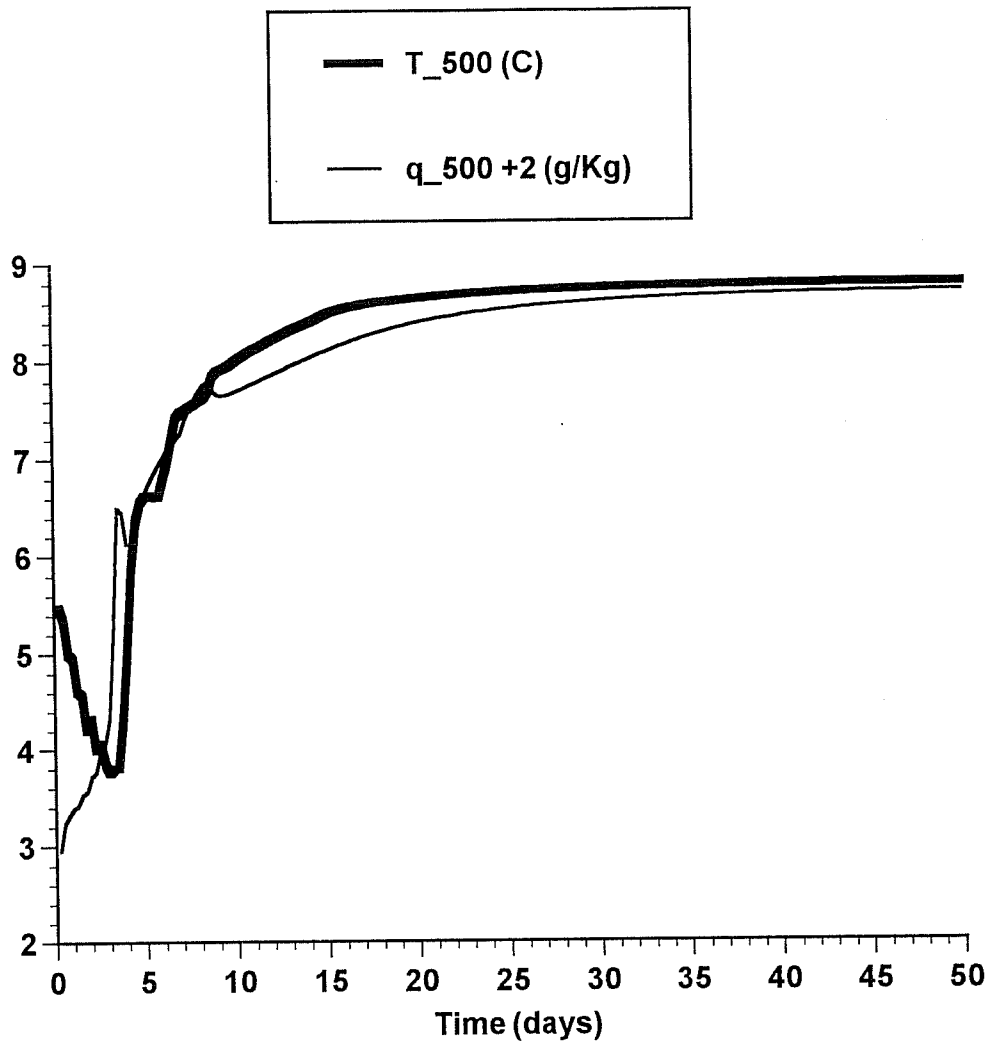

Fig. 3 Adjustment of 500-mb temperature (heavy line; °C) and specific humidity (thin line; gm/kg +2) toward radiative-convective equilibrium, beginning from an arbitrary initial state.

equilibrium. There is an initial, rapid adjustment of the 500-mb temperature (not shown), followed by a much slower evolution of both the temperature and specific humidity fields over about a 20-day time scale. Clearly, it will be necessary to integrate a single-column model over at least 20 days to allow the scheme to come into equilibrium with the large-scale conditions.

Figure 4 shows an example of a 31-day average comparison of relative humidity predicted by a single-column model forced with TOGA-COARE IFA data versus the corresponding observed relative humidity. The root-mean-square relative humidity error accumulated in time is of order 25%, up to 300 mb. (The rawinsonde-derived relative humidities are not reliable above 300 mb.) The convection scheme in this run has not been optimized in any way. It is important to note that the comparisons of Q_1, Q_2, and precipitation to those derived directly from budget analysis of the data are nearly "perfect" in the sense that the fields look very similar, once again confirming the lack of validity of using Q_1, Q_2, or precipitation as means of evaluating convection schemes.

In the following section, I describe in some detail a particular convection scheme that will be

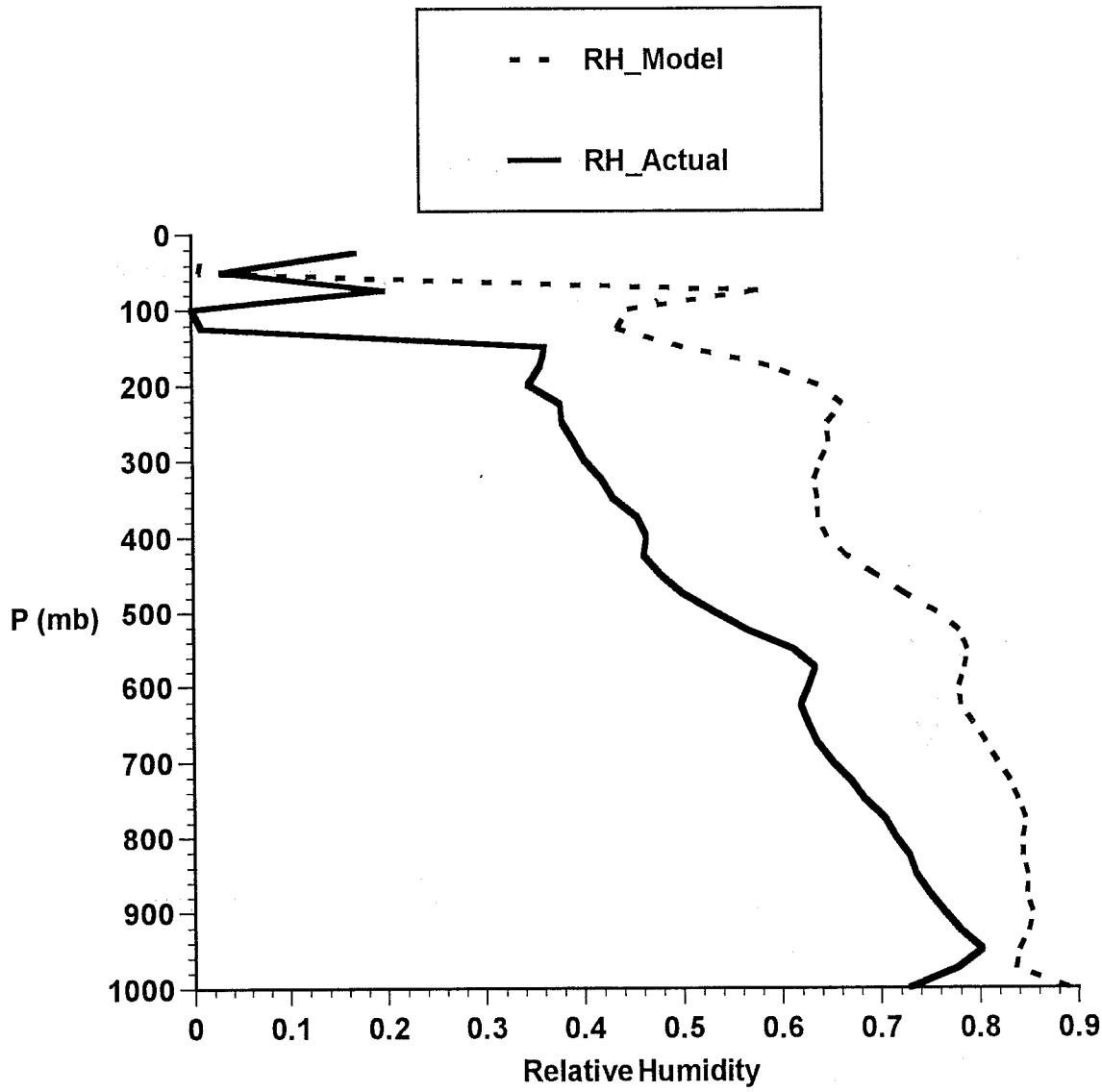

Fig. 4 The relative humidity predicted by an unoptimized convective scheme driven by observed forcing as deduced from the TOGA-COARE Inner Flux Array (dashed) versus the observed relative humidity (solid). Both quantities have been averaged over the month of December 1992.

used to explore the sensitivity of humidity prediction to cloud microphysics.

4. A NEW CONVECTION SCHEME

The new scheme described here is a modification of one described previously by the author (Emanuel, 1991). It is based on the idea of episodic (rather than continuous) mixing in cumulus clouds, as first proposed by Raymond and Blyth (1986) and having received considerable support from analysis of aircraft observations inside clouds (e.g., Taylor and Baker, 1991).

First consider the entire convective updraft-only mass flux through cloud base, M. This quantity is regulated in the scheme according to the hypothesis that convection keeps the subcloud air neutrally buoyant with respect to the air just above the top of the subcloud layer (but not necessarily with

respect to air above that level). Thus the very simple closure for M is given by

$$\frac{\partial M}{\partial t} = \alpha \left(T_{\rho p} - T_\rho\right)_{\mathrm{ICB}} - \beta M, \tag{4.1}$$

where α and β are constants, T_ρ is the density temperature of the environment, $T_{\rho p}$ is that of a reversibly lifted parcel, and the subscript ICB denotes the first model level above cloud base. The last term in (4.1) is a small damping term to stabilize the integration.

A fraction δM_i of the undilute cloud base mass flux mixes with the environment at each level i. (We will discuss momentarily what happens to the resulting mixtures.) The rate of environmental mixing is not at present well determined by observations, but we follow the general conclusions of Bretherton and Smolarkiewicz (1989) by postulating that the rate of mixing is proportional to the change with height of buoyancy of undilute cloud air. Specifically, we postulate that

$$\delta M_i = M \left[\frac{|\delta B_i| + \lambda \delta p_i}{\sum_i \left[|\delta B_i| + \lambda \delta p_i \right]} \right], \tag{4.2}$$

where δB_i is the rate of change with height of undilute parcel buoyancy at level i, δp_i is the pressure thickness of layer i, and λ is a constant. Thus the rate of mixing of undilute air is a constant added to a weighting depending on how rapidly undilute buoyancy changes with height.

At each level i, an amount of undilute cloud air, δM_i, mixes with its environment at that level, forming a spectrum of mixtures containing different amounts of environmental air, after a fraction ϵ_i of the adiabatic condensed water has been converted to precipitation. Each mixture then ascends or descends to a new model level, j, at which the mixture is neutrally buoyant with respect to its environment. (Note that for some mixtures, $j = i$.) A fraction, ϵ_j, of the condensed water in each such mixture is converted to precipitation.

In principle, each mixture at level j should then be allowed to mix again with environment, with each secondary mixture again ascending or descending to its level of neutral buoyancy. But this gets to be computationally demanding, and so we truncate the mixing tree after the first round of mixing. Another compromise that we make is to detrain the mixed samples not exactly at their levels of neutral buoyancy, but instead at levels where the liquid water virtual static energy (2.3) of the mixture is the same as that of its environment. This insures that the detrained air will always be neutrally buoyant once it has mixed with enough of the environment that any remaining condensed water has evaporated.

All the precipitation that forms is added to a single precipitation shaft, part of which is assumed to fall back down through the cloud (and thus not to suffer any evaporation) and part of which, a specified areal fraction σ_s, is assumed to fall through the ambient environment and to be subject to evaporation. The cooling by evaporation is assumed to yield a hydrostatic downdraft whose mass flux is governed by the rate of evaporation and the ambient stratification. This unsaturated downdraft

entrains mass from or detrains mass to the environment, depending on the sign of the vertical gradient of its mass flux. (See Emanuel, 1991, for details.) The unsaturated downdraft advects heat and moisture through the atmosphere.

The tendencies of temperature and specific humidity produced by the scheme are given by the rate of compensating subsidence, the detrainment of water substances from the cloud and unsaturated downdraft, the evaporation of precipitation, and a myriad of small effects such as downward heat advection and frictional dissipation in precipitation particles. These are necessary to ensure exact conservation of vertically integrated enthalpy by the scheme.

In experiments with a single-column model driven by TOGA COARE data, it was discovered that it is important to directly couple the convective downdraft to the surfaces fluxes. The convective downdrafts enhance the surface fluxes by increasing the grid-area average surface wind speed, and by producing a negative correlation between fluctuations in wind speed and fluctuations of temperature and specific humidity. Output from the convective subroutine allows one to incorporate these effects in the large-scale model.

After some experimentation, it was found that good predictions of relative humidity can be obtained using a specification of precipitation efficiencies, ϵ_i, that mimics the Kessler warm-rain autoconversion process, but with an autoconversion threshold that is temperature dependent. Thus the ϵ_i's are specified such that all condensed water above a threshold amount, $l_{\rm crit}$, is converted to precipitation, with $l_{\rm crit}$ given by

$$l_{\rm crit} = \begin{cases} l_0 & \text{for } T > 0°\text{C}, \\ l_0 \left(1 - \frac{T}{T_{\rm min}}\right) & \text{for } T_{\rm min} \le T < 0°\text{C}, \\ 0 & \text{for } T < T_{\rm min}. \end{cases} \tag{4.3}$$

Thus the autoconversion threshold decreases linearly with temperature between the freezing level and $T_{\rm min}$.

With this specification, Table 1 summarizes all of the important adjustable parameters of the convection scheme.

As can be seen, the number of adjustable parameters is moderately large. Predictions of relative humidity prove sensitive to most of these, except the strictly numerical parameters, as long as they lie within a fairly broad range of values. The sensitivity of predictions of relative humidity to assumptions about cloud microphysics was described by Rennó et al. (1994). The next section outlines a procedure for optimizing these parameters and evaluating the scheme.

5. OPTIMIZATION AND EVALUATION OF CONVECTIVE SCHEMES

The large sensitivity of relative humidity predictions to the way convection is represented provides an opportunity to optimize convective schemes by adjusting the parameters to yield an optimum

Table 1. Adjustable parameters

Name	Description
l_0	Maximum autoconversion condensed water threshold
$T_{\rm min}$	Minimum temperature (C) below which the autoconversion threshold is zero
$V_{\rm rain}$	The terminal velocity of rain (m s^{-1})
$\omega_{\rm snow}$	The terminal pressure velocity of snow (mb s^{-1})
$c_{\rm rain}$	A coefficient governing the rate of evaporation of rain
$c_{\rm snow}$	A coefficient governing the rate of evaporation of snow
σ_s	The fractional of precipitation falling into ambient air
σ_d	The fractional area covered by the unsaturated downdraft
λ	The entrainment constant (see text)
$\sigma_{\rm SL}$	The fraction of the subcloud layer assumed to be affected by convective outflows
Numerical parameters	
α	Coefficient governing the rate of approach to subcloud-layer equilibrium (see 4.1)
β	The rate of damping in the approach to subcloud-layer equilibrium (see 4.1)

humidity forecast in the single-column model. To the extent that the parameters are universal, the scheme should be optimized for all conditions. Naturally, not all the parameters will be universal and so a true test of the scheme is to run the optimized single-column model using data collected under very different conditions (e.g., a polar outbreak over relatively warm ocean) and then to evaluate its prediction of relative humidity. At the time of this writing, we have performed the first of these two steps, using data from the TOGA-COARE Inner Flux Array (IFA) provided by Richard Johnson of Colorado State University. This CSU data provides all the bracketed quantities in (3.1)–(3.2) needed for the single-column prediction, except for the surface fluxes and radiation. The surface fluxes are provided through the standard bulk aerodynamic formulae, modified to account for the enhanced surface fluxes owing to convective downdrafts. The sea surface temperature is updated every six hours. Radiation is calculated using the radiative transfer code developed by Chou et al. (1991). At present, clear skies are used in the radiative transfer code; we plan to incorporate a representation of fractional cloudiness soon.

Many runs of the single-column model were made and the parameters optimized to produce the best possible prediction of relative humidity during the month of December 1992. The resulting averaged relative humidity is shown as a function of pressure in Figure 5, which can be compared to the pre-optimized prediction for the same month in Figure 4. The root-mean-square error for relative humidity over the 31 days and from the surface to 300 mb is about 14%, compared to 25% for the pre-optimized scheme. Experiments are now being done to assess what part of the remaining error is due to errors in the data used to force the single-column model, versus remaining errors in the convective scheme. The next step, which remains to be taken, is to drive the optimized scheme with

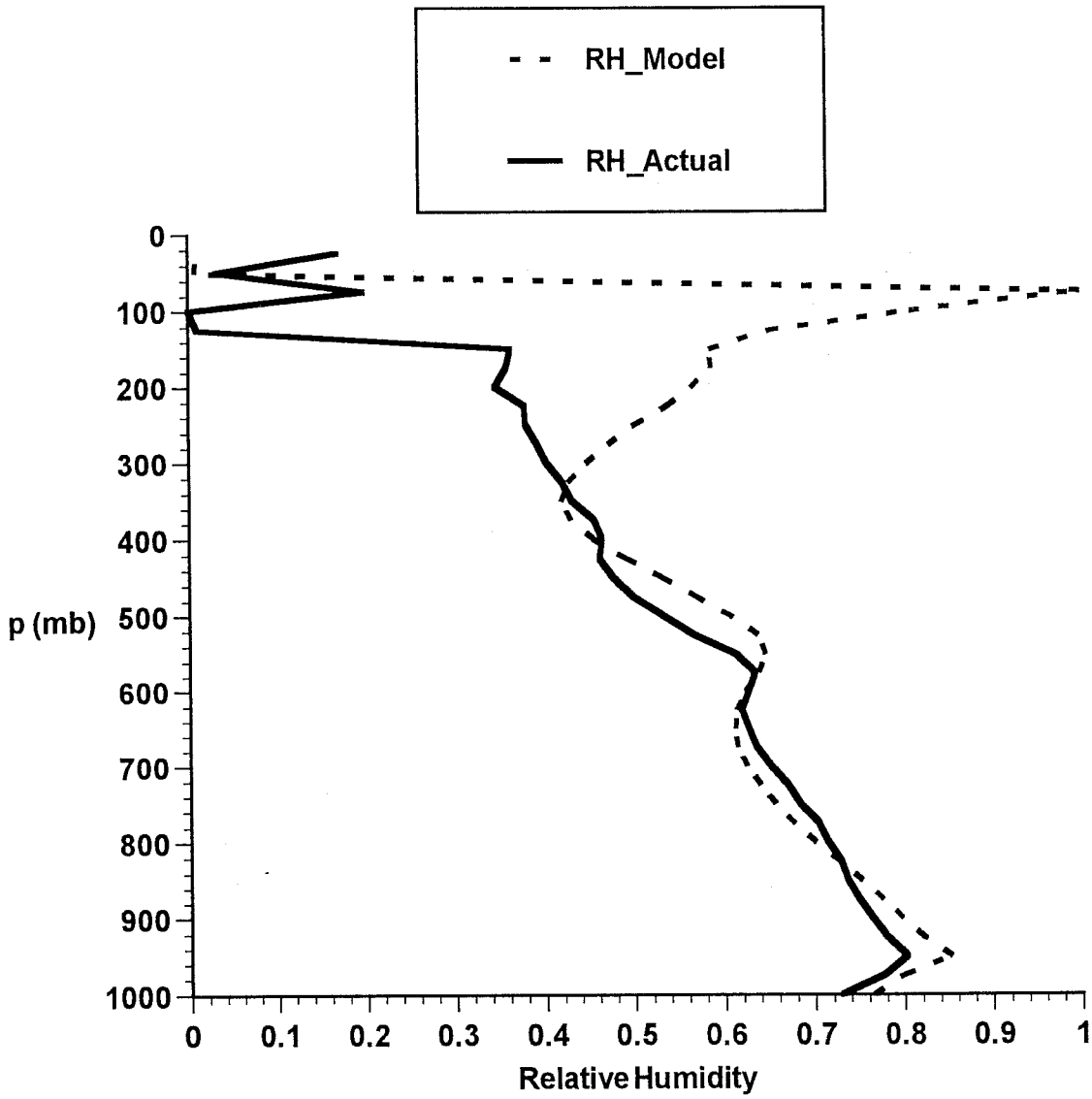

Fig. 5 The relative humidity predicted by the optimized convective scheme run in a single-column model driven by observed forcing as deduced from the TOGA-COARE Inner Flux Array (dashed) versus the observed relative humidity (solid). Both quantities have been averaged over the month of December 1992. Note that observed relative humidities are not reliable above 300 mb.

an independent data set, to assess the overall performance of the scheme. Figure 6 does, however, show the results of using November 1992 TOGA-COARE data. The prediction of relative humidity is still quite good.

The vertical resolution of the single-column model and the data used to drive it is 25 mb. Figure 7 shows the results of degrading the resolution to 50 mb and to 100 mb. The 100-mb resolution run produces very bad results, and the relative humidity prediction ceases to be very sensitive to the cloud microphysics parameters. The dominant water balance in the coarse resolution run shown in Figure 7 is between drying by subsidence and moistening by upward numerical diffusion. These results are consistent with those found by Sun and Oort (1995), who showed that there is a strong correlation between fluctuations in relative humidity at the surface and humidity at virtually all levels

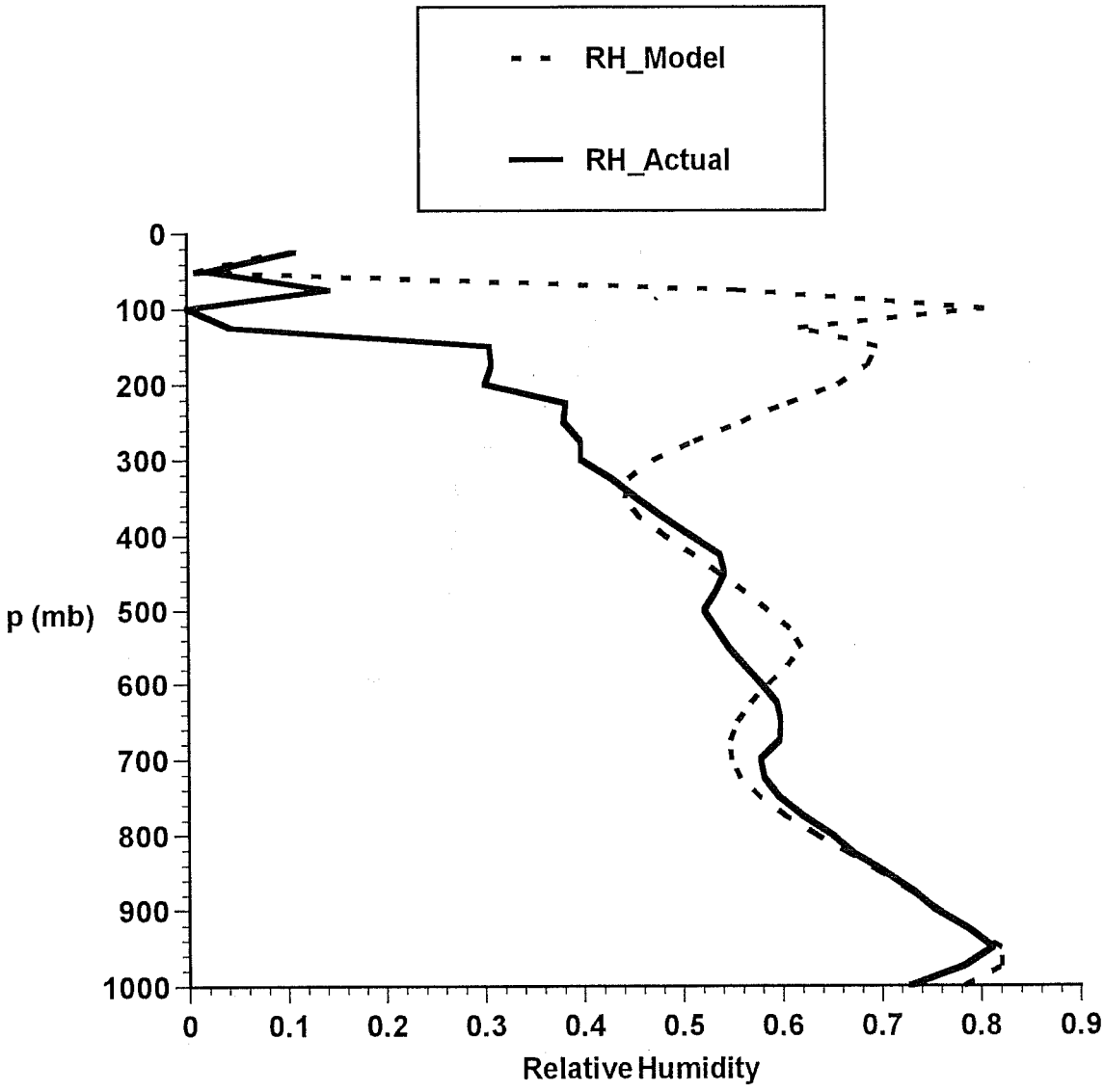

Fig. 6 Same as Figure 5, but for November 1992.

in the troposphere in GCM's, while in nature, the correlation decays rapidly with altitude. Taken together, these results plausibly explain why the water vapor feedback in virtually all climate models is nearly the same in spite of their employment of greatly differing convective schemes: the model water balance critically involves upward numerical diffusion of water, masking the real sensitivity to convective cloud microphysics. While modelers may be tempted to argue that sensitivity to cloud microphysics is exaggerated in single-column models, horizontal advection of water cannot eliminate the sensitivity of atmospheric water vapor content to variability in the source of water vapor, which is detrainment from clouds and evaporation of precipitation.

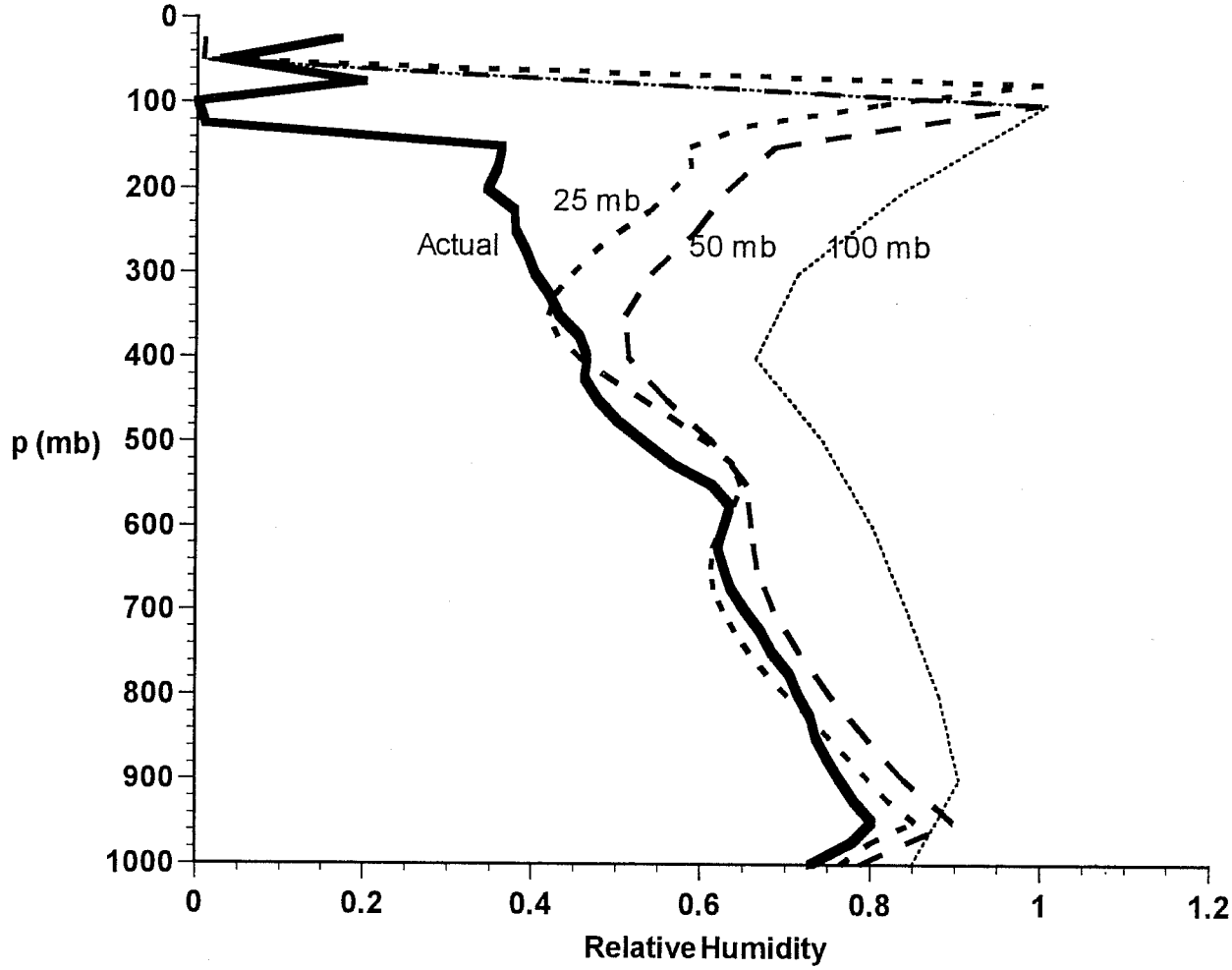

Fig. 7 The solid and short-dashed lines are the same fields as displayed in Figure 5, while the heavy dashed and dotted lines represent relative humidity predicted by the single-column model with vertical resolution degraded to 50 mb and 100 mb, respectively. Other experiments with 100-mb resolution in which microphysical parameters were varied produced results nearly indistinguishable from the dotted line shown here.

6. SUMMARY

The water vapor content of the troposphere depends sensitively on the magnitude of the sources of water in detrainment from clouds and evaporation of precipitation. Experiments with high-resolution single-column models demonstrate this sensitivity but also show that the sensitivity is masked by numerical diffusion if the vertical resolution is too coarse. Resolution of at least 50 mb appears to be necessary to properly handle water vapor. Standard tests of convective schemes, such as semi-prognostic tests and comparisons of observed with predicted precipitation, are virtually useless for properly evaluating the fidelity with which such schemes simulate heating and moistening by convective clouds, because the actual tendencies represent fractionally very small differences between adiabatic and radiative cooling and convective heating. An alternative method is to predict the evolution in time of a truly sensitive predictand such as relative humidity, using a single-column model driven by observed forcing. Such a prediction must be carried out over a period of time at least

as large as the adjustment time of water vapor, typically about 20 days. Such predictions readily reveal flaws in the convection scheme and provide an opportunity to optimize and evaluate the scheme. We should strive to devise more tough tests for our parameterizations and avoid the temptation to "validate" schemes by subjecting them to easy tests designed to cast them in the best possible light.

7. REFERENCES

Bretherton, C. S., and P. K. Smolarkiewicz, 1989: Gravity waves, compensating subsidence and detrainment around cumulus clouds. *J. Atmos. Sci.*, **46**, 740–759.

Chou, M.-D., D. P. Krats and W. Ridgway. 1991: Infrared radiation parameterization in numerical climate models. *J. of Climate*, **4**, 424–437.

Emanuel, K. A., 1991: A scheme for representing cumulus convection in large-scale models. *J. Atmos. Sci.*, **48**, 2313–2335.

Lord, S. J., 1982: Interaction of a cumulus cloud ensemble with the large-scale environment. Part III: Semiprognostic test of the Arakawa-Schubert cumulus parameterization. *J. Atmos. Sci.*, **39**, 88–103.

Raymond, D. J., and A. M. Blyth, 1986: A stochastic model for nonprecipitating cumulus clouds. *J. Atmos. Sci.*, **43**, 2708–2718.

Rennó, N. O., Emanuel, K. A., and P. H. Stone, 1994: Radiative-convective model with an explicit hydrological cycle, Part I: Formulation and sensitivity to model parameters. *J. Geophys. Res.*, **99**, 14429–14441.

Sun, D.-Z., and A. H. Oort, 1995: Humidity-temperature relationships in the tropical troposphere. *J. Climate*, **8**, 1974–1987.

Taylor, G. R., and M. B. Baker, 1991: Entrainment and detrainment in cumulus clouds. *J. Atmos. Sci.*, **48**, 112–121.

Yanai, M., S. Esbensen, and J.-H. Chu, 1973: Determination of bulk properties or tropical cloud clusters from large-scale heat and moisture budgets. *J. Atmos. Sci.*, **30**, 611–627.